International Journal of Microwave and Wireless Technologies, 2014, 6(3/4), 313–324.
doi:10.1017/S1759078714000415

RESEARCH PAPER

A 94-GHz planar orthogonal mode transducer

JAWAD ATTARI[1], TAREK DJERAFI[2] AND KE WU[2]

The orthogonal LSM_{10} and TE_{10} modes that are supported by the image SINRD (iSINRD) guide and substrate integrated waveguide *(SIW) is exploited to develop a planar millimeter-wave hybrid orthogonal-mode transducer (OMT) within the same dielectric substrate. The two output arms are iSINRD guide and an SIW. The proposed co-layered planar OMT belongs to a narrowband acute angle class. The design process is explained and measurements at 94 GHz are presented. No septa or step changes in thickness are required. Both modes are excited using WR10 transitions, where the transition of one mode is orthogonal to the other. Therefore, the OMT is fabricated as a back-to-back 4-port OMT; two inputs and two outputs for each mode respectively. The lateral dimensions of all guiding arms are 0.6 × 0.635 mm². An insertion loss of around 1.2 dB is obtained for both LSM_{10} and TE_{10} modes, while isolation better than 17 dB is obtained for both modes (30 dB for the LSM_{10} mode).*

Keywords: iSINRD guide, SIW, Orthogonal-mode transducer (OMT), NRD guide, Millimeter-wave circuits, Substrate integrated circuits (SICs)

Received 20 October 2013; Revised 26 February 2014; Accepted 27 February 2014; first published online 3 April 2014

I. INTRODUCTION

Recent years have witnessed an exponential growth in millimeter-wave circuits such as couplers, filters, and ortho-mode transducers (OMTs), to name a few. The latter is especially interesting for millimeter-wave applications, where two signals of opposite polarities can be transmitted or received using a single channel.

Although the OMT is a three-port device, from a physical point of view, it is nonetheless comprised four electrical ports. This is due to the fact that the input physical port receives or transmits two electrically orthogonal modes or signals, and can thus be viewed as two separate electrical ports. This is better understood when looking at Fig. 1, which shows the *S*-matrix (representing a four-port circuit such as the OMT which, electrically speaking, is a four-port circuit) and schematic representation of a typical ideal OMT circuit [1]. Although both reflection and isolation should be minimized, reducing the latter is of utmost importance as, in the context of OMT's, it would signify cross-talk or cross-polarization between the two orthogonal modes.

A lot of research effort has been invested toward conceiving planar millimeter-wave components that can be seamlessly integrated within a complete communication system [2–6]. The OMT, however, stands out as an exception owing to a multitude of reasons, chief among which is the original role of the OMT as polarization splitter. Because the signals to be separated by the OMT are of different polarization, the geometry of the OMT always contains two planes (mostly *E* and *H* planes). Alternatively, while a planar design is possible [1], it is only feasible if septa are embedded in each of the output arms; in this case the septa would be aligned in different planes. In either case, it is a daunting task at millimeter-wave frequencies, given the minute lateral circuit dimensions that are in the order of less than one millimeter. Furthermore, a common problem encountered in millimeter-wave circuits design is the difficulty of conceiving them using micro-strip or co-planar waveguide, due to substantially higher losses

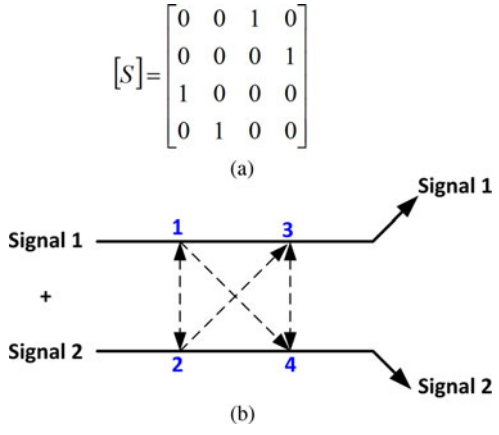

Fig. 1. (a) The *S*-matrix, and (b) the schematic representation of an OMT circuit, assuming an electrical four-port OMT configuration. Numbers in blue: the (electric) port numbers. Dashed arrows: minimal cross-polarization interference.

[1]BlackBerry Ltd., Waterloo, N2L 3W8, Canada. Phone: +1 514 340 4711
[2]École Polytechnique de Montréal, Montréal, H3T 1J4, Canada
Corresponding author:
J. Attari
Email: jawad.attari@polymtl.ca

and dimensional limitations associated with millimeter-wave frequencies [2].

Instead of the use of dielectric waveguides such nonradiative dielectric (NRD) waveguides were proposed [7]. Nevertheless, such waveguides have the problem of mechanical stability, which is easily circumvented using substrate integrated NRD (SINRD) waveguide, or the recently proposed, more compact image SINRD (iSINRD) guide [8]. The latter has the advantages, besides size compactness, of suppressing all even modes as well as possessing a versatile geometry. Those advantages encourage the use of the iSINRD guide in hybrid circuits. In this work, a planar iSINRD–substrate integrated waveguide (SIW) OMT is proposed, in which all sections lie in one plane only and no embedded septa are required. In Section II, the design principles are outlined. Simulated and measured results are then presented in Section III. The OMT is designed to operate at 94 GHz.

II. OVERVIEW OF ORTHO-MODE TRANSDUCES

From a physical perspective, OMTs are three-port power dividers whose operating principle resembles that of duplexers [1]. However, from an electrical point of view, the OMT is a four-port device, since the input port of the OMT is always designed to support two orthogonal signals. Many OMT configurations and classes exist in the literature [1], and their choice between them is subject to technical requirements and specifications, as well as fabrication limitations [1].

The distinguishing feature of the OMT as a power divider is its ability to divide or combine two distinct signals of different polarization into or from separate ports with little cross-polarization interference between the two. Hence transmit and receive (or uplink and downlink) communication can take place simultaneously, since the transmit and receive ports are perfectly isolated. For this reason, OMTs are used in satellite communications and radar systems as well as radio astronomy applications. OMTs differ from diplexers in that they split and combine signals at the same frequency band, whereas diplexers typically handle signals of different frequencies [1].

To support simultaneous uplink and/or downlink transmission of orthogonally polarized signals, an OMT is always designed with a common waveguide section that supports, at the same frequency, two signal modes of orthogonal polarizations. This common waveguide is always followed by a splitting section (sometimes called a turnstile junction) which precedes the two output ports (or transmit/receive ports in some applications), and its design principle varies depending on the application. This turnstile junction gradually separates the two combined signals into the ports that support their propagation. Therefore, the two signal ports are geometrically different.

In most OMT designs, the common waveguide is a square waveguide that supports the TE_{10} and TE_{01} modes, whereas the signal ports are rectangular waveguides that are geometrically the reverse of each other [1]. A lot of geometrical manipulation is then required to gradually separate the two signals. In some designs, an *H*-plane waveguide is connected to the common *E*-plane waveguide to separate one of the two signals [1, 9]. If a planar design is a strict requirement, septa can be introduced in the signal arms that help isolate the two signals [1, 10], but this comes at the expense of significantly less bandwidth [11]. In either case, some degree of manipulation of the common waveguide is always required in order for the two orthogonal signals to be separated to their respective output ports with minimal cross-polarization interference. These manipulations become increasingly difficult at millimeter-wave frequencies.

A lot of research efforts have been invested to minimize the complexity of OMT design at millimeter-wave frequencies, such as the symmetric reverse-coupling 100-GHz OMT reported in [9], and the 35-GHz OMT for correlation receivers, described in [12]. Despite the fact that they do not contain embedded septa, and no thickness tapering is required within a single plane, their design still requires the two output ports to be in orthogonal planes. Furthermore, their design is based on the rectangular waveguide which cannot easily implemented in planar circuits, and which exhibits more pronounced attenuation per unit length at higher millimeter-wave frequencies.

In the next sections, the traditional mechanical limitations of the OMT design at millimeter-wave frequencies (septa, thickness tapering, dual-plane design, and rigid waveguide design) are completely eliminated by virtue of intuitive use of a novel guiding structure as well as strategic implementation of orthogonal modes and boundary conditions.

III. A PROPOSED NOVEL OMT DESIGN

The only way to avoid thickness tapering of, or usage of septa in the output arms of the OMT, while still maintaining the planar architecture, is for the output OMT arms to be realized as different waveguides. Each of these different waveguides would then support only one of the two orthogonal modes, despite having the same thickness. This means that the common channel should then support both orthogonal modes at the same frequency, and the turnstile regions should be designed in a special way such that it can split the modes into their respective output arms without the need to resort to thickness tapering or implementation of septa.

The best planar alternative to the rectangular waveguide that can be easily integrated in planar circuits is the SIW. However, the above preposition would not be feasible with the SIW because it can practically support only the TE_{10} mode; the orthogonal TE_{01} mode would leak from the metallic via posts. Furthermore, although it is amenable to integration in planar systems, the use of the SIW does not eliminate the need for either septa or dual-plane design, since it is otherwise not possible to split the TE_{10} and TE_{01} modes, unless the thickness is changed in one of the output arms.

Fortunately, other guiding structures have been developed for millimeter-wave applications. One such waveguide is the NRD waveguide [7, 13], which is simply a dielectric strip placed between two metal covers, with the sides being regions of air; in other words, regions of parallel plates. Thus as long as frequency of operation is less than the cut-off of parallel plates modes [7], no modes are excited in the sides and the wave is well contained in the dielectric strip. Like the rectangular waveguide, its planar version is the SINRD guide [2], where the air regions are realized as perforation air via holes. Depending on the mode of operation, the more compact and versatile iSINRD guide can instead be used, which is half the size of the SINRD guide, thanks

https://doi.org/10.1017/S1759078714000415 Published online by Cambridge University Press

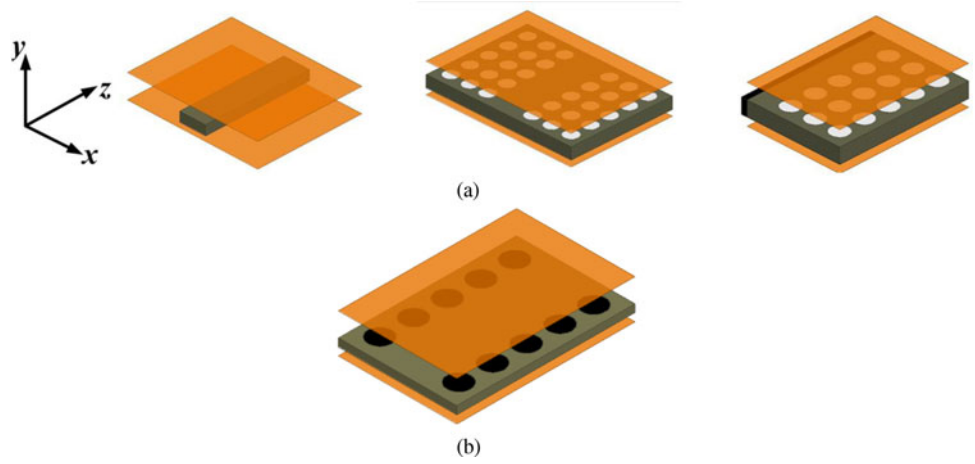

Fig. 2. The 3D views of the (a) NRD guide (left), SINRD guide (center), and iSINRD guide (right) and (b) the SIW. Orange: metal covers, green: dielectric, white: air vias, and black: image metal plane of the iSINRD guide or metal via holes of the SIW.

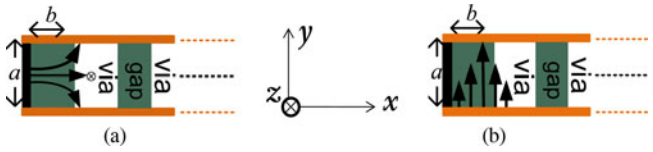

Fig. 3. The cross-sectional front view of the *E*-field lines of the LSM_{10} (left) and TE_{20} (right) modes in the iSINRD guide. The × represent the E_z component of the LSM_{10} mode.

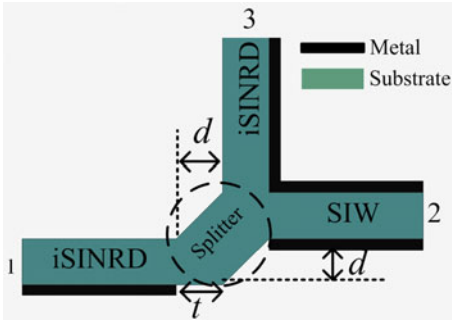

Fig. 4. Top view of the proposed iSINRD–SIW OMT.

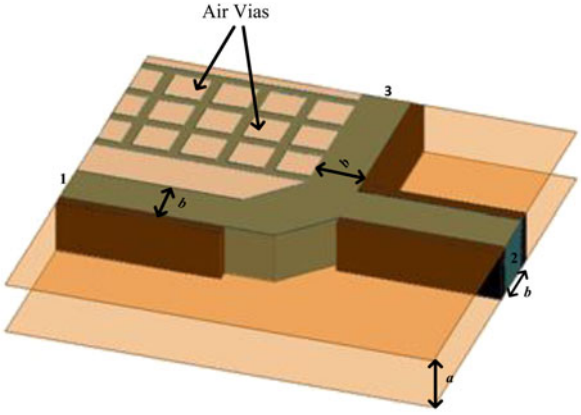

Fig. 5. A 3D view of the proposed iSINRD–SIW OMT with the lateral dimensions of each arm. White: air vias, orange: metal covers, black: metal planes, and green: substrate.

to a metal image plane that facilitates the size reduction [8, 13, 14]. The set of modes supported by the three NRD variants are identical, except for the ones that are suppressed by the image metal plane in the iSINRD guide.

From a physical point of view, the only difference between the SIW and the iSINRD guide is the fact that the latter has only one metallic edge instead of two as in the SIW; the other side is a region of reduced permittivity (compared to that of the central guide). The NRD guide and its two planar versions are shown in Fig. 2(a), whereas the SIW is shown in Fig. 2(b).

The two guides, however, differ in the class of modes that they support. Although the SIW is technically limited to the *TE* modes only (*TM* modes are not supported since the side metal walls are not continuous), the iSINRD has a wider range of supported modes. Furthermore, it can support the fundamental TE_{10} mode of the SIW, in addition to a host of other modes of orthogonal polarization, such as the LSM_{10} mode. The two modes are shown in Fig. 3. It is important to mention that the TE_{10} mode supported in the iSINRD guide is actually the second order of the TE_{10} mode in the rectangular guide or the SIW (i.e. it is the TE_{20} mode), because the image metal plane of the iSINRD guide suppresses the fundamental TE_{10} mode [14], along with other symmetric *TE* modes. Also, while the TE_{20} mode has an *E* component in the *y*-plane only, the LSM_{10} mode has all three components. It is important to mention that the E_z component of the LSM_{10} mode must be zero at the center of the guide (i.e. $x = 0$ or at the metal image plane). For this reason, the LSM_{10} mode continues to exist in the iSINRD guide despite the presence of the image metal plane [14].

These facts about the LSM_{10} mode and the TE_{20} mode in the iSINRD guide facilitate the design of a planar OMT that

https://doi.org/10.1017/S1759078714000415 Published online by Cambridge University Press

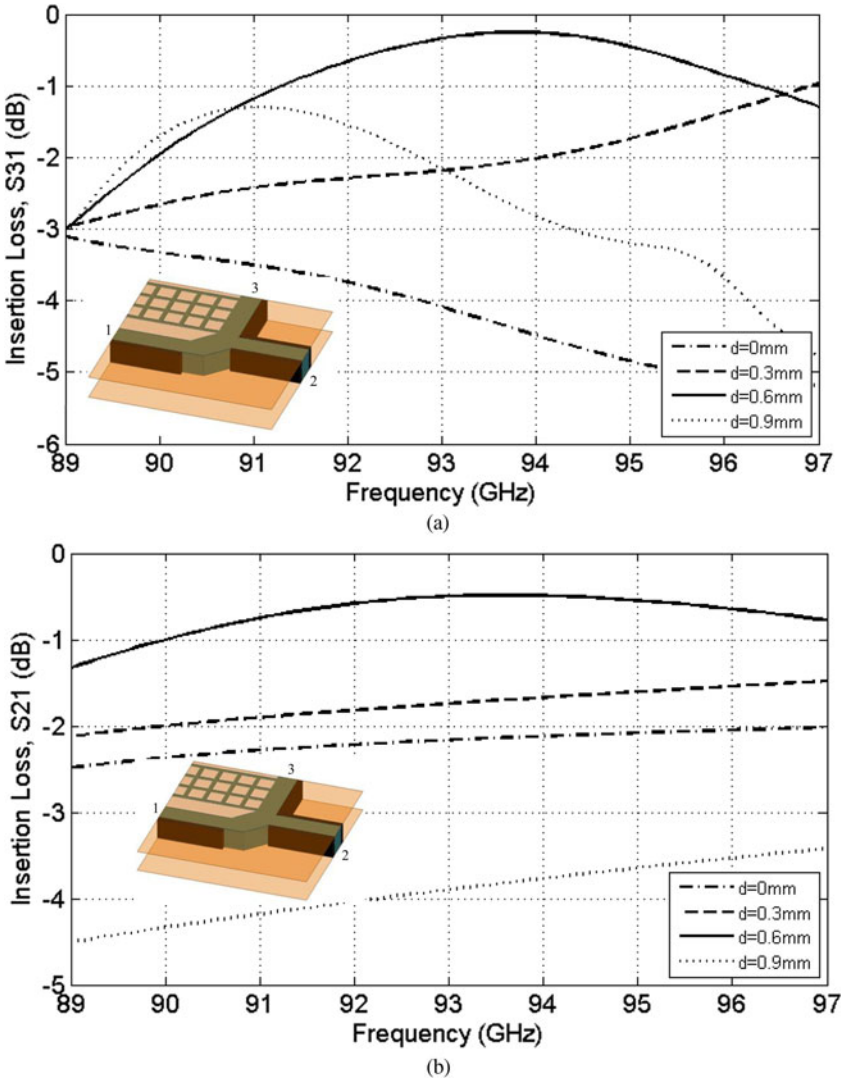

Fig. 6. The relationship between the insertion loss and different values of d for (a) the LSM_{10} mode and (b) the TE_{10} mode.

has all its components lying in the same plane and that does not require any further modification of the output arms as would typically be required in traditional OMT designs. The detailed E-field equations of the two modes in the dielectric and side regions can be found in [7, 14]. Further detailed analyses of the two guides, including analysis of the attenuation and propagation, can be found in [8] and [14].

IV. MECHANISM OF THE PROPOSED OMT

A) The geometry of the proposed OMT

The top and three-dimensional (3D) view of the proposed OMT is shown in Fig. 4. Its common channel is an iSINRD guide that supports the propagation of the orthogonal LSM_{10} and TE_{20} modes. The former mode is collected at an iSINRD guide output arm, whereas the latter is separated into an SIW output arm. The common channel and the output arms are separated by a tapered splitter region that facilitates the separation of the two modes into their respective arms. The splitter region does not have metal wall on either side. In other words, the splitter region is essentially an SINRD guide. Hence, there will be no radiation or diffraction from the central splitter region because, as aforementioned, radiation is suppressed in the side regions of the SINRD guide as long as the operating frequency is less than that of parallel plate modes (of the side regions). The parameter d control the length and width of the taper, whereas the parameter t controls the length of the metal side plane of the iSINRD guide common channel into the splitter region. In the special case where $d = 0$, the width of the taper equals the width of the iSINRD and the SIW; if they are equal. According to [14], the cut-off of the LSM_{10} mode primarily depends on the thickness of the substrate, a, rather than the width which is mainly responsible for the bandwidth [14]. On the other hand, the cut-off of the TE_{10} mode in the SIW depends only on the width, b [15]. Thus, to reduce the complexity of the design, the width of both guides ought to be equal. For an operational bandwidth centered at 94 GHz, based on Alumina substrate ($\varepsilon_r = 9.8$, $\tan\delta = 10^{-4}$ at 94 GHz [16]), the optimum width for both modes is $b = 0.6\ \lambda_g$, while the substrate thickness should be $a = 0.635\ \lambda_g$

https://doi.org/10.1017/S1759078714000415 Published online by Cambridge University Press

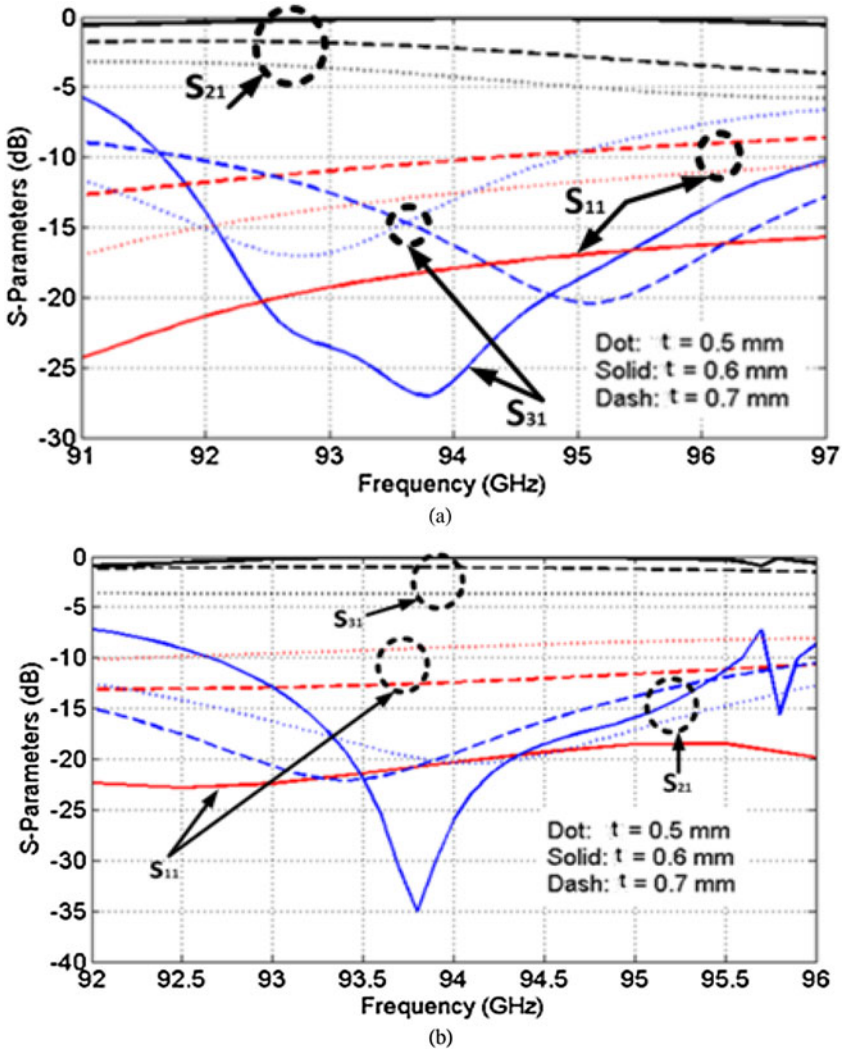

Fig. 7. The effect of inset distance t on the S-parameters of (a) the TE_{10} mode and (b) the LSM_{10} mode. Black: transmission; red: reflection; blue: isolation.

[14]. This value ensures a single mode operation for both the LSM_{10} mode (until 102 GHz [14]) and the TE_{10} mode (until 150 GHz) Fig. 5.

B) Mode separation

The OMT then works as follows. For the LSM_{10} mode, since the E_z component must be null at the metal plane, the LSM_{10} mode cannot propagate into the SIW arm (port 2), and it will simply continue to the iSINRD arm (port 3). This is similar to the mechanism of the cruciform coupler described in [17], and in fact, for this mode, any value of d or t can be used, even $d = t = 0$. For the TE_{20} mode, the splitter converts it into the TE_{10} mode which, as mentioned earlier, is not supported by the iSINRD guide, since its metal side plan will suppress it. Therefore, it cannot propagate into the iSINRD guide output arm, and will instead propagate into SIW output arm where it is supported.

The parametric curves in Fig. 6, plot the transmission level of both modes as a function of frequency for different values of d, and confirm that $d = 0.6$ mm corresponds to optimum transmission. The value of t is then optimized using [18] and according to Fig. 7, $t = d = 0.6$ mm for optimum transmission and isolation. As is apparent, excellent separation of the two modes can be achieved with the above mechanism without introducing any septa or thickness changes, and without requiring different planes to separate the two modes. This is confirmed by the 3D E-field plot of the two modes shown in Fig. 8. Note that as established in [14], the air region in the iSINRD guide can be represented by a PMC plane to save simulation time.

The different dimensions of the OMT established thus far can further be verified by simulating the two splitter segments shown in the insets of Figs 9 and 10. The first segment represents the feeding dual-mode arm of the OMT and half of the splitter region, whereas the second segment represents the other half of the splitter leading to the two output single-mode arms. The simulated S-parameters shown in Figs 9 and 10 indicate that the chosen dimensions correspond to optimum matching of the OMT sections and serve as a good verification to the splitter dimensions. Note, however, that those results are based on the assumption that the modes exactly in the middle of the splitter are pure LSM_{10} and TE_{10} modes. In reality, a hybrid of the two modes exists in the splitter due to their simultaneous feed to the input arm. The orthogonality of the two modes, however, ensures minimal interference, and the S-parameters

https://doi.org/10.1017/S1759078714000415 Published online by Cambridge University Press

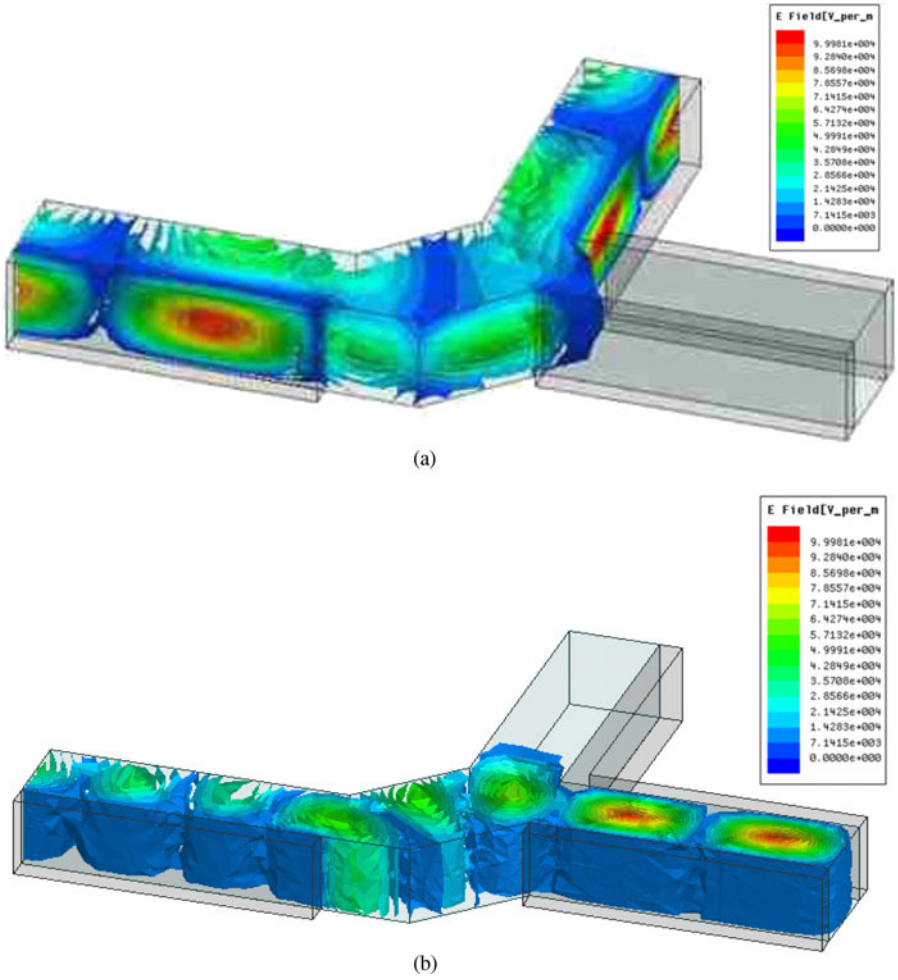

Fig. 8. A 3D plot of the *E*-field of (a) the LSM_{10} mode and (b) the TE_{20} mode in the iSINRD–SIW OMT.

in Figs 9 and 10 are thus valid for the hybrid case. Although other higher-order modes maybe excited, they are largely suppressed by the metallic walls of the iSINRD and SIW guides. They could further be suppressed if a metallic septum is introduced in the middle of the splitter region. Alternatively, the electromagnetic bandgap (EBG) structure mode suppression technique detailed in [19] could theoretically be employed. Those two mode suppression techniques, however, are not feasible at 94 GHz, and it suffices to use the metal planes of the iSINRD and SIW guides as mode suppressors.

C) Exciting the orthogonal modes

Given the high-target frequency (94 GHz), the use of microstrip or coplanar waveguide (CPW) excitation is impractical for the dimensions determined above. Alternatively, the tapered transition to WR10 has been the most frequently used excitation method of the LSM_{10} and TE_{10} modes in SINRD and SIW circuits, respectively [13, 19]. The schematic views and dimensions of the WR10 transitions for the two modes are shown in Fig. 11. The dimensions of the non-WR10 waveguide sections of the transitions were optimized using [18]. Note that, in the case of the LSM_{10} mode, the WR10-waveguide transition has the same height but different lengths and widths. Conversely, for the TE_{10} mode, the WR10-waveguide transition have the same width and length but different heights.

Since the two modes (and their WR10 feeding transitions) are orthogonal, the proposed iSINRD–SIW OMT cannot be fabricated as a three-port device. Instead, the OMT approach in [20–22] is employed, where the three-port OMT is fabricated back-to-back so that it has four ports; two of which act as feeding ports for the LSM_{10} and TE_{10} modes. Hence, conflict in mode excitation is avoided since each mode is being fed separately. The suggested four port OMT, and field plot of simultaneous feed, are shown in Figs 12(a) and 12(b), respectively. The "common channel" is thus an iSINRD guide that supports both (superposed) modes. In other words, actual OMT input port starts from the common channel, with mode separation into ports 3 and 4 taking place in the splitter on the right. The feed to the iSINRD arms is realized by tapering the substrate into the WR10 guide transition. On the other hand, the feed to the SIW arms is simply achieved by extending the substrate into the WR10 guide. Probe dimensions were optimized using [18]; lengths of the iSINRD taper and the SIW probe are 1 and 0.6 mm, respectively. The four-port OMT together with the feeding waveguides are shown in Fig. 12(c).

D) Fabrication

The OMT is fabricated on Alumina ($\varepsilon_r = 9.8$) substrate. As aforementioned, feeding of the LSM_{10} and TE_{10} modes is

https://doi.org/10.1017/S1759078714000415 Published online by Cambridge University Press

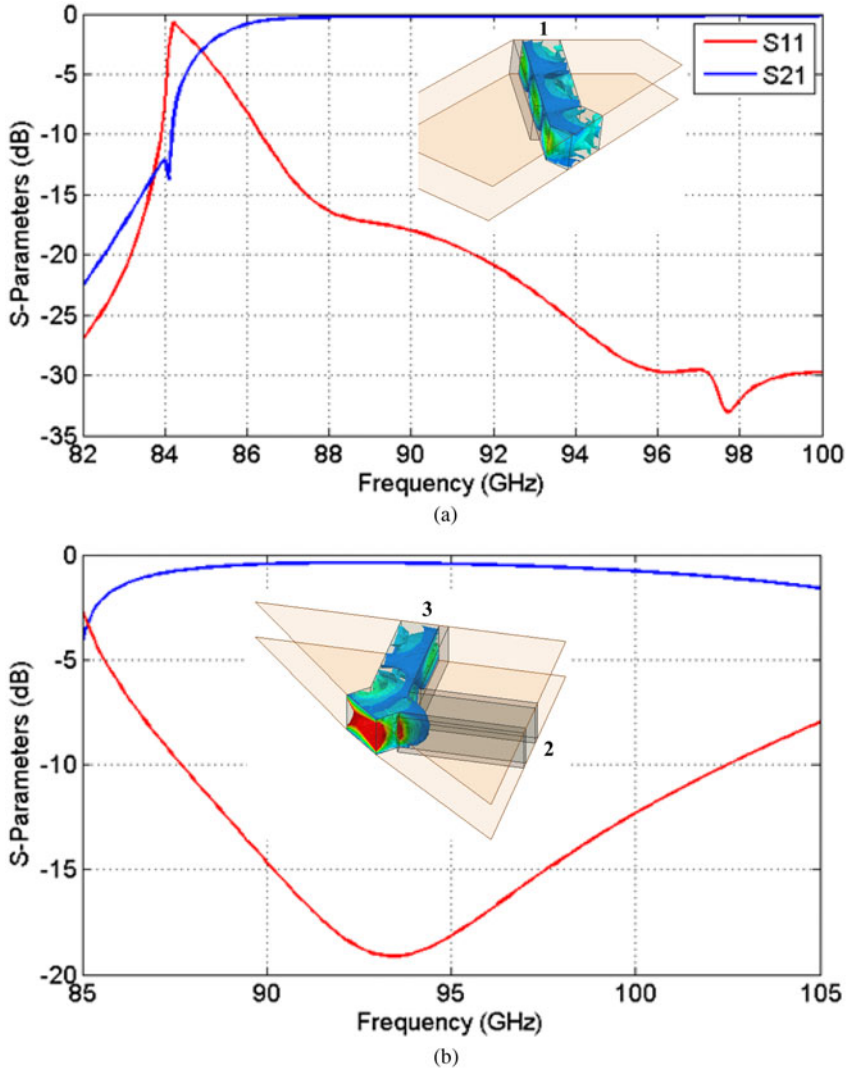

Fig. 9. The *S*-parameter response of the LSM_{10} mode in the (a) first splitter segment and (b) the second splitter segment. Insets: the *E*-field of the LSM_{10} mode in each segment.

done by virtue of a tapered transition to WR10 waveguide as detailed above. The regions adjacent to the iSINRD arms were perforated using square (0.5×0.5 mm^2) air vias. The dimensions were chosen to satisfy the non-radiating criteria of the LSM_{10} mode, given by $f_x = c/(2a\sqrt{\varepsilon_2})$, where f_x and ε_2 are the cut-off of the parallel-plate mode in, and permittivity of, the side region, respectively [14].

All metallic walls are realized by the aluminum cavity metal. The reason being that metalizing via holes in alumina substrate with the MHMIC technique is not yet a mature process at our lab and is mostly unsuccessful.

Unlike the LSM_{10} mode, which can still be contained in the dielectric despite some substrate perforation, the TE_{20} mode requires an intense perforation that renders the iSINRD guide an iNRD guide. Otherwise, the TE_{20} mode easily leaks into the side region. Therefore, an iSINRD circuit that involves operation with the TE_{20} mode must have its sections that support the TE_{20} mode realized as an iNRD guide. For example, the field plots in Figs 13(a) and 13(b) of an iNRD and iSINRD guide bends, respectively, illustrate this idea. It is clear from the two plots that the TE_{20} mode would leak if the substrate perforation is involved, such as the case in an iSINRD guide bend. Conversely, an iNRD guide bend would contain the TE_{20} mode well with no leakage. Therefore, air vias were avoided in the common central channel to prevent leakage of the TE_{10} mode in the side region (See Fig. 12).

V. MEASUREMENT RESULTS

The fabricated prototype is shown in Fig. 14, together with the aluminum base within which the transition is realized. Measurements were made separately for the LSM_{10} and TE_{10} modes due to the vector network analyzer (VNA) being limited to two ports only. In other words, one input and one output ports were connected to the VNA at the same time, and loads were used to match the other ports. Prior to the measurements, standard thru-reflect-line (TRL) calibration was used to dembed the effect of the WR10 transition and the substrate tapers.

Simulated and measured results of the OMT are shown in Figs 15(a) and 15(b) for the LSM_{10} and TE_{10} modes, respectively. In both cases, an insertion loss of around 1 dB is obtained at the frequency of operation (94 GHz), which

https://doi.org/10.1017/S1759078714000415 Published online by Cambridge University Press

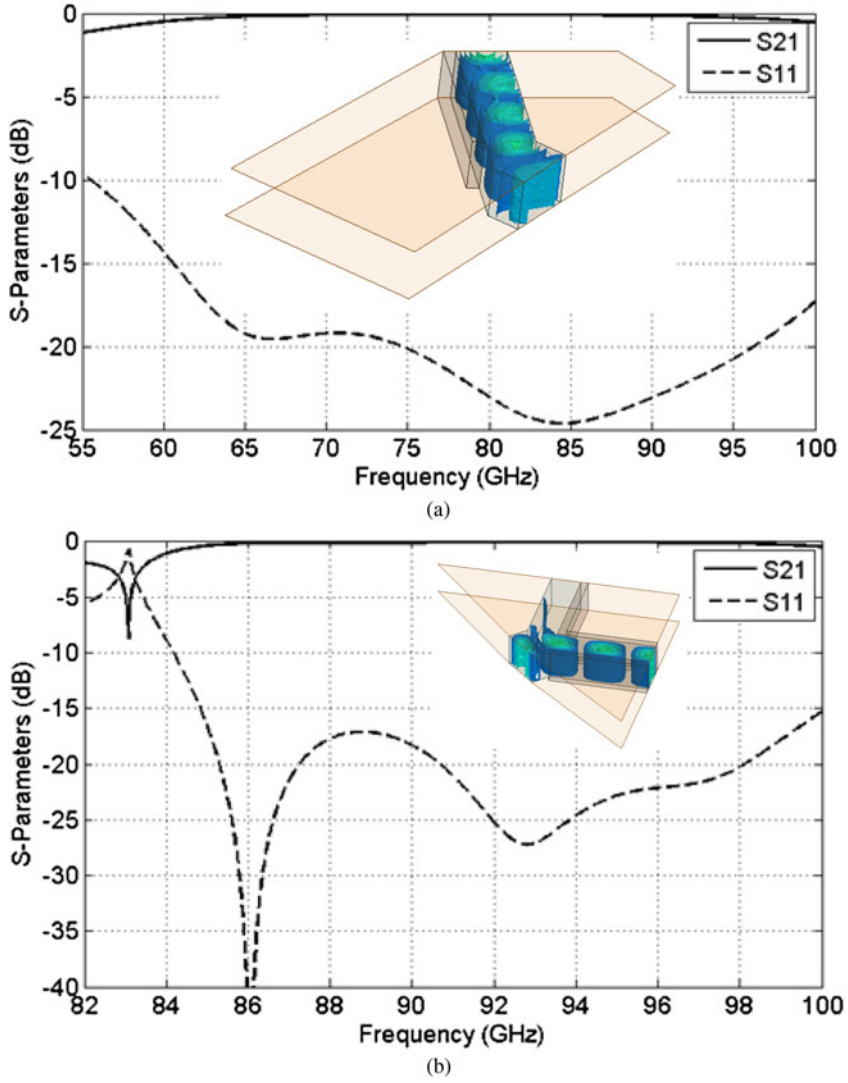

Fig. 10. The *S*-parameter response of the TE_{10} mode in the (a) first splitter segment and (b) the second splitter segment. Insets: the *E*-field of the TE_{10} mode in each segment.

includes the metal and dielectric losses (the latter being rather negligible given the low tanδ of Alumina, as verified in [7, 16]). A return loss of around 17 dB was obtained as well for both modes. The isolation for the LSM_{10} mode is 30 dB) and that of the TE_{10} mode is 17 dB at 94 GHz. The measured isolation level is very good and, in general, good agreement is observed between the simulated and measured results over the measured bandwidth which is around 6.5%.

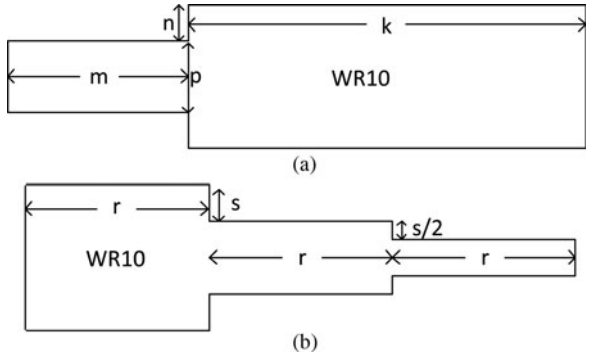

Fig. 11. (a) Top view and (b) side view of the WR10 transitions used to excite the LSM_{10} and TE_{10} modes respectively. $k = 10.16$ mm, $m = 2.89$ mm, $n = 0.2175$ mm, $p = 0.835$ mm, $s = 0.1588$ mm, $r = 5$ mm. Note: the diagrams are not to scale.

For the two modes, the return loss is rather constant over the measured bandwidth, with an average of 20 dB for the LSM_{10} mode and 17 dB for the TE_{10} mode. On the other hand, the response of the cross-mode isolation is narrowband. This is because the cross-mode isolation is dependent on how well the splitter is able to sustain the conversion of each mode in the common channel to that which is desired to be exclusively supported by one of the output arms. Evidently, this process is frequency dependent, and can only be attained over a fraction of the measured bandwidth.

VI. CONCLUSION

This paper proposes a novel millimeter-wave planar OMT circuit comprised iSINRD guide and SIW, which are made in co-layered substrate. The design is motivated by the fact that the fundamental modes of the two waveguides are

https://doi.org/10.1017/S1759078714000415 Published online by Cambridge University Press

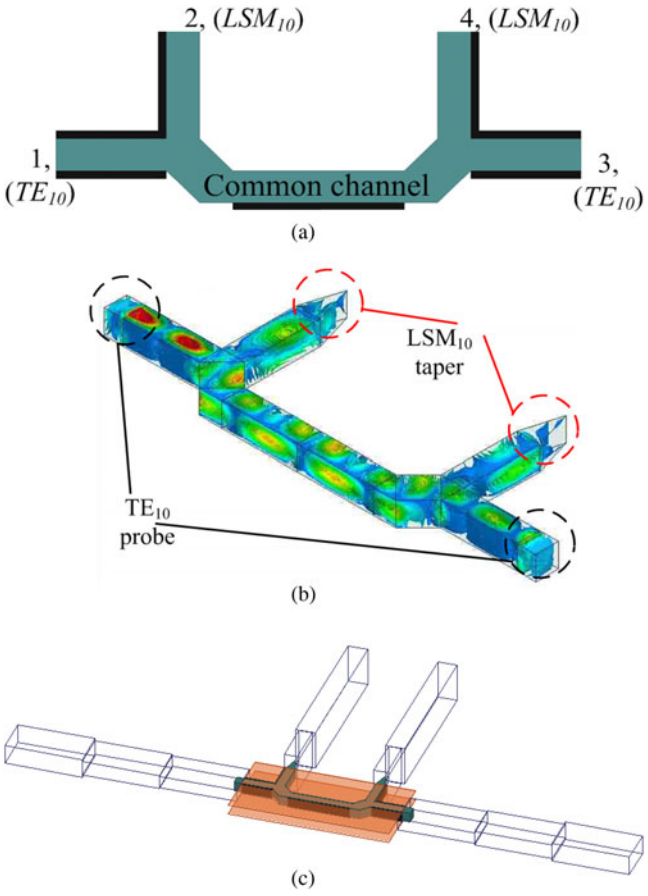

Fig. 12. The back-to-back four-port iSINRD–SIW OMT: (a) A top view of the back to back, four-port iSINRD–SIW OMT, and (b) Field plot of the four-port OMT, with simultaneous LSM_{10} and TE_{10} feed (top left corner). Notice the excellent separation at the output branches. (c) The four-port OMT together with the transition to the WR10-waveguide transitions.

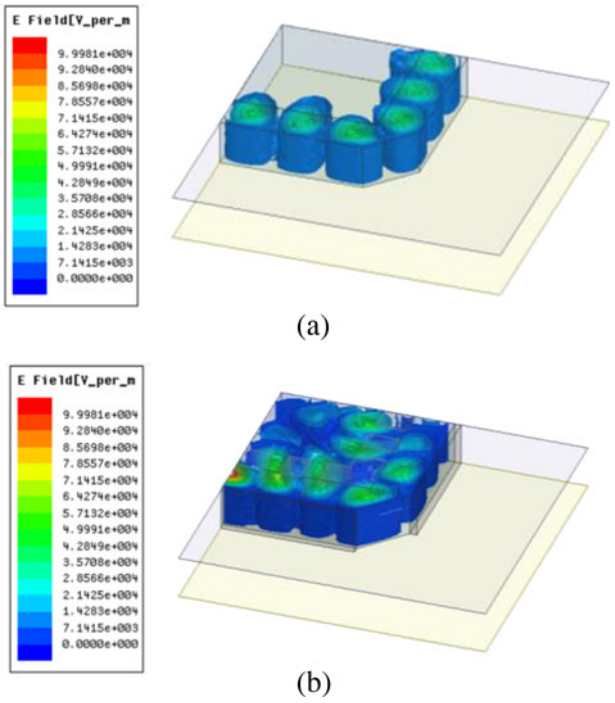

Fig. 13. 3D field plots in which: (a) The LSM_{10} mode is well contained in the guide when the side region is purely air, and (b) The TE_{20} mode easily leaks into the side region if it is perforated.

mutually orthogonal, and that the iSINRD guide can support the propagation of the TE_{10} mode as well as the LSM_{10} mode. Hence, with a correct choice of dimensions of the iSINRD guide and the SIW, a simple planar multi-waveguide OMT circuit can be conceived. Neither septa nor thickness tapering of the output branches are required in this setup. The OMT is fabricated as a back-to-back four-port OMT, in order to facilitate the excitation of both the LSM_{10} and TE_{10} modes. Measurements agree well with the theory, which confirms the validity of the proposed hybrid OMT.

The return and insertion losses have a rather flat response over the measured bandwidth compared to the cross-mode isolation. This points to the fact that the

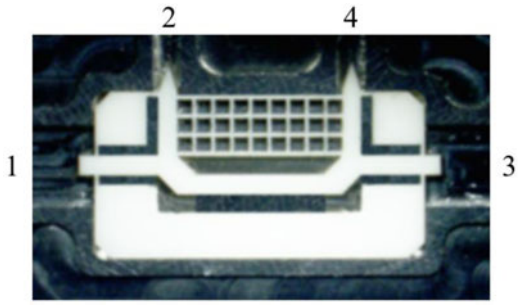

Fig. 14. The fabricated four-port iSINRD–SIW OMT.

https://doi.org/10.1017/S1759078714000415 Published online by Cambridge University Press

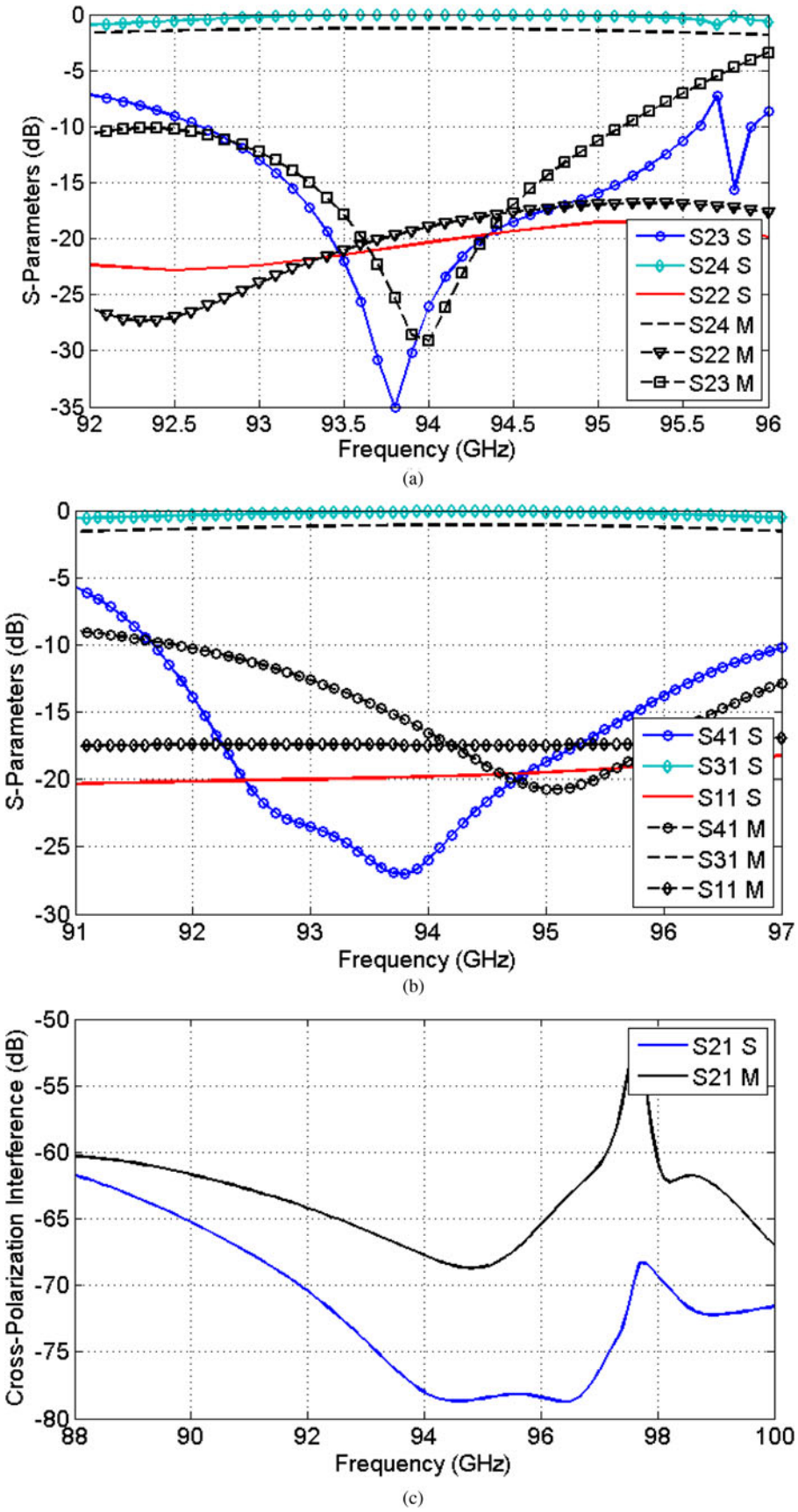

Fig. 15. Simulated (S, color) and measured (M, black) *S*-parameters for (a) the LSM_{10} and (b) the TE_{10} mode, as well as the (c) cross-polarization interference between the LSM_{10} and TE_{10} modes.

https://doi.org/10.1017/S1759078714000415 Published online by Cambridge University Press

mode separation function of the splitter is frequency dependent, at least for the splitter topology proposed in this work. Further investigation of the splitter regions is thus required in order to improve the bandwidth of the cross-mode isolation. In addition, an in-depth modal analysis of modes in the splitter region is also considered for the future work.

REFERENCES

[1] Uher, J.; Bornemann, J.; Rosenberg, U.: Waveguide Components for Antenna Feed Systems: Theory and CAD, Chapter 3, Artech House, Boston, London

[2] Wu, K.; Deslandes, D.; Cassivi, Y.: The substrate integrated circuits – a new concept for high-frequency electronics and optoelectronics, 6th TELSIKS, 2003.

[3] Wu, K.: Integration and interconnect techniques of planar and non-planar structures for microwave and millimeter-wave circuits – current status and future trend, in Asia Pacific Microwave Conf.2, vol. 2, 2001, 411–416.

[4] Deslandes, D.; Wu, K.: Integrated microstrip and rectangular waveguide in planar form. IEEE Microw. Wirel. Compon. Lett., **11** (2) (2001), 68–70.

[5] Cheng, Y., Hong, W.; Wu, K.: Half mode substrate integrated waveguide (HMSIW) directional filter. IEEE Microw. Wirel. Compon. Lett., **17** (7) (2007), 504–506.

[6] Patrovsky, A., Wu, K.: Substrate integrated image guide (SIIG) – a low-loss waveguide for millimetre-wave applications, in 35th European Microwave Conf., vol. 2, 2005.

[7] Koul, S.K.: Millimeter Wave and Optical Dielectric Integrated Guides and Circuits, Chapter 6, J. Wiley & Sons, New York, 1997.

[8] Attari, J.; Djerafi, T.; Wu, K.: Fast simulation of millimeter wave components using commercial software. IEEE Microw. Mag., **14** (2) (2013), 106–111.

[9] Navarrini, A.; Nesti, R., Symmetric reverse-coupling waveguide orthomode transducer for the 3-mm band. IEEE Transact. MTT, **57** (1) (2009), 80–88.

[10] Chattopadhyay, G.; Philhour, B.; Carlstrom, J.E.; Church, S.; Lange, A.; Zmuidzinas, J.: A 96-GHz ortho-mode transducer for the polatron. IEEE Microw. Guid. Wave Lett., **9** (9) (1999), 421–423.

[11] Chattopadhyay, G.; Carlstrom, J.E.: Finline ortho-mode transducer for millimeter waves. IEEE Microw. Guid. Wave Lett., **9** (9) (1999), 339–341.

[12] Peverini, O.A.; Tascone, R.; Virone, G.; Olivieri, A.; Orta, R.: Orthomode transducer for millimeter-wave correlation receivers. IEEE Transact. Microw. Theory Tech., **54** (5) (2006), 2042–2049.

[13] Bahl, B.: Millimeter Wave Engineering and Applications, Chapter 5, J. Wiley & Sons, New York, 1984.

[14] Al Attari, J.: Innovative Millimeter-wave Components Based on Mixed Substrate Integrated Dielectric-Metallic Waveguides. PhD thesis, Ecole Polytechniqe de Montreal, 2013.

[15] Deslandes, D.; Wu, K.: Design consideration and performance analysis of SIW components, in 32nd European Microwave Conf., 2002, 1–4.

[16] Afsar, M.N.: Precision millimeter-wave dielectric measurements of birefringent crystalline sapphire and ceramic alumina, instrumentation and measurement. IEEE Transactions on, **IM–36** (2) (1987), 554–559.

[17] Attari, J.; Djerafi, T.; Wu, K.: A compact 94 GHz image substrate integrated non-radiative dielectric (iSINRD) waveguide cruciform coupler. IEEE Microw. Wirel. Compon. Lett., **23** (10) (2013), 533–535.

[18] Ansys HFSS ver. 13.0, ANSYS Inc., Canonsburg, PA, 2011.

[19] Cassivi, Y.; Wu, K.: NRD-guide spurious mode suppressor using self-contained periodic planar EBG structure, in Asia Pacific Microwave Conf., vol. **2** (2011), 659–662.

[20] Moldovan, E.; Bosisio, R.G.; Wu, K.: W-band multiport substrate-integrated waveguide circuits. IEEE Transact. Microw. Theory Tech., **54** (2) (2006), 625–635.

[21] Tao, Y.; Shen, Z.; Liu, G.: Equivalent circuit model of square waveguide T-junction for ortho-mode transducers, in IEEE MTT-S Int. Microwave Symp. Digest, 2009.

[22] Tao, Y.; Shen, Z.; Liu, G.: Closed-form expressions for the equivalent circuit model of square-waveguide T-junctions and its application in OMT design. IEEE Transact. Microw. Theory Tech., **58** (5) (2010), 1167–1174.

Dr. Jawad Attari received his B.Eng. degree in Electrical Engineering from Sultan Qaboos University, Muscat, Oman, in 2004 and the M.Sc. degree in Communications Technology from Universität Ulm, Ulm, Germany in 2008. He recently obtained his Ph.D. degree in Electrical Engineering in 2013 from the École Polytechnique de Montréal. He won the first prize of the Student Design Competition of the IMS2012 in Montreal, and a Best Paper Certificate of Recognition at the EuMC, Nuremberg 2013. He is currently working as an RF Design at BlackBerry Product Development Center in Waterloo, Ontario, Canada, where he designs the complete RF Front-end of the BlackBerry smartphones. His current research interests include nonlinear RF circuits design; envelop tracking techniques, as well as antenna design for smartphones.

Dr. Tarek Djerafi received the Dipl.Ing. degree from the Institut d'Aeronautique de Blida, Blida, Algeria, in 1998, the M.A.Sc. and Ph.D. degrees in Electrical Engineering from École Polytechnique, Montreal, QC, Canada, in 2005 and 2011, respectively. He is currently a Post-Doctoral Fellow with the École Polytechnique, Montreal. He has authored or co-authored more than 30 papers in journals and conferences. His current research interests include telecommunication antennas, beam forming networks, and radio frequency components design. Dr. Djerafi was the recipient of the NSERC Post-Doctoral Fellowship in 2011, selected for the Industrial R&D Fellowships Program in 2011, and for the FQNRT-CREER International Bourse in 2009 for his short-term Visiting Scholar in LAAS-CNES, Toulouse, France. He is currently serving as a Technical Reviewer for the IEEE-MTT, the IEEE Microwave and Wireless Components Letters Progress in Electromagnetic Research, IET Microwaves, and a Project Evaluator for the Romanian Research Council.

https://doi.org/10.1017/S1759078714000415 Published online by Cambridge University Press

Prof. Ke Wu is professor of electrical engineering and Tier-I Canada Research Chair in RF and millimeter-wave engineering at the Ecole Polytechnique (University of Montreal). He holds the first Cheung Kong endowed chair professorship (visiting) at the Southeast University, the first Sir Yue-Kong Pao chair professorship (visiting) at the Ningbo University, and an honorary professorship at the Nanjing University of Science and Technology, the Nanjing University of Post Telecommunication, and the City University of Hong Kong, China. He has been the Director of the Poly-Grames Research Center. He was the founding Director of the Center for Radiofrequency Electronics Research of Quebec (Regroupement stratégique of FRQNT) for 2008–2014. He has also hold guest and visiting professorship at many universities around the world. He has authored or co-authored over 960 referred papers, and a number of books/book chapters and filed more than 30 patents.

https://doi.org/10.1017/S1759078714000415 Published online by Cambridge University Press